

Continuous Flow Synthesis of Azoxybenzenes by Reductive Dimerization of Nitrosobenzenes with Gel-Bound Catalysts

Carsten J. Schmiegel,^[a] Patrik Berg,^[a] Franziska Obst,^[b] Roland Schoch,^[a]
Dietmar Appelhans,^[b] and Dirk Kuckling*^[a]

In the search for a new synthetic pathway for azoxybenzenes with different substitution patterns, an approach using a microfluidic reactor with gel-bound proline organocatalysts under continuous flow is presented. Herein the formation of differently substituted azoxybenzenes by reductive dimerization of nitrosobenzenes within minutes at mild conditions in good to almost quantitative yields is described. The conversion within the microfluidic reactor is analyzed and used for optimizing and validating different parameters. The effects of the different

functionalities on conversion, yield, and reaction times are analyzed in detail by NMR. The applicability of this reductive dimerization is demonstrated for a wide range of differently substituted nitrosobenzenes. The effects of these different functionalities on the structure of the obtained azoxyarenes are analyzed in detail by NMR and single-crystal X-ray diffraction. Based on these results, the turnover number and the turnover frequency were determined.

Introduction

Flow reactors are useful tools to enable continuous organic reactions. Important benefits of flow reactions are the direct use of immobilized catalyst within a continuous flow system and the permanent synthesis of catalyst-free product^[1] which can be easily isolated by solvent evaporation. Flow reactors also allow an online detection of reactions^[2] and adjustments to the reaction parameters even while the reaction is already running.^[3] Especially for microfluidic reactors (MFRs) with smaller dimensions, further advantages such as excellent heat exchange and a laminar flow can be observed.^[4] Additional advantages of MFRs are the small amounts of chemicals needed. Thus using highly reactive or toxic components such as nitroso- or azoxy compounds becomes easily possible.^[5] This is especially beneficial considering safety aspects as well as considerations regarding the high and growing status of "green chemistry" within modern chemical research.^[6–8]

To enlarge the catalytic activity inside the flow reactor, catalysts can be integrated within crosslinked polymer networks. Using relatively low crosslinker contents enables reactions inside of swollen, sponge-like, polymer networks, which, in contrast to solid particles, increases the amount of immobi-

lized and accessible catalyst from only surface area to bulk volume.^[9] The general applicability of surface-bound gels with a high crosslinker content as carriers of catalysts and enzymes in MFRs, has already been shown recently.^[10,11] In both cases, hexagonally ordered gel arrays, immobilized on glass slides, were obtained via photolithography, and used for various reactions within MFRs. For a high contact of the educt solution with the polymer gel, hexagonally arranged gel arrays prove to be an efficient basic structure. The necessary fast and efficient production of complex polymer gel-based microfluidic chips on glass substrates can be achieved via a one-step photostructuring.^[12] Based on such arrays immobilization of tertiary amines as catalysts in surface-bound gels is also possible and offers access to a wide range of Knoevenagel reactions under continuous flow conditions.^[11]

To double down on the general use of hexagonally ordered gel dot arrays in MFRs, the aim of this study was to integrate proline as a versatile organo-catalyst,^[13] in gel dot arrays for the reductive dimerization of toxic and highly reactive nitrosobenzenes to azoxyarenes, (Figure 1). Therefore, the applicability of this organic reaction under mild conditions was tested for the synthesis of symmetric and asymmetric azoxyarenes.

Azoxyarenes are valuable building blocks carrying an uncommon oxygen-nitrogen-nitrogen, presenting a 1,3-dipolar, moiety.^[14] In recent years the interest in preparing azoxybenzene compounds increased drastically due to their versatile properties in applications to liquid crystals,^[15] polymer materials, stabilizers, and analytical reagents.^[16,17] Additional attractive properties of azoxybenzenes especially for medical as well as synthetic chemists are the retinoidal activities^[18] and the opportunity to act as o-directing group in C–H-functionalizations of arenes.^[19] Furthermore, the azoxy functionality can be seen as a bioisoster for amide and alkene functions and thus shows promising anti-cancer activities as the corresponding bioactive amides and alkenes.^[20]

[a] C. J. Schmiegel, P. Berg, Dr. R. Schoch, Prof. Dr. D. Kuckling
Department of Chemistry, Faculty of Science, Paderborn University
Warburger Str. 100, 33098 Paderborn, Germany
E-mail: dirk.kuckling@uni-paderborn.de
<https://chemie.uni-paderborn.de/arbeitskreise/organische-chemie/kuckling>

[b] Dr. F. Obst, Dr. D. Appelhans
Leibniz Institute for Polymer Research Dresden
Hohe Str. 6, 01069 Dresden, Germany

Supporting information for this article is available on the WWW under <https://doi.org/10.1002/ejoc.202100006>

© 2021 The Authors. European Journal of Organic Chemistry published by Wiley-VCH GmbH. This is an open access article under the terms of the Creative Commons Attribution License, which permits use, distribution and reproduction in any medium, provided the original work is properly cited.

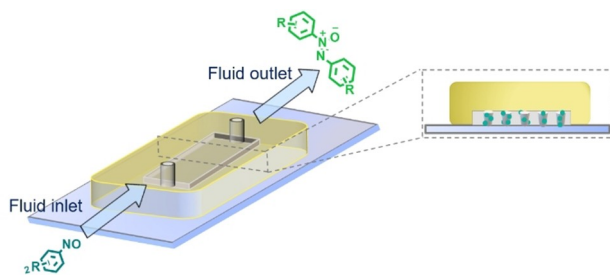
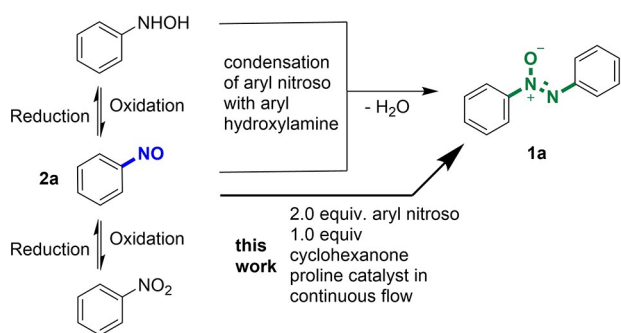


Figure 1. General setup of polymer network immobilized organocatalysts inside of a microfluidic reactor. The liquid supply could be realized via a syringe pump as shown in Figure S3. The gel points immobilized on the glass substrate with an attached catalyst are covered with a prefabricated PTFE reactor shape with defined recesses. As a result, the dwell time inside the reactor can be precisely adjusted using the syringe pump. In the detailed view along the direction of flow, the green spheres represent the immobilized organocatalyst within the gel structures.

Usually, the preparation of azoxybenzenes proceeds via condensation of aryl nitroso compounds with aryl hydroxylamines.^[21] Consequently, this synthesis strategy involves the oxidation of anilines or the reduction of nitroaromatics, respectively, to obtain the two constituents of the subsequent condensation (Scheme 1). Exemplary for this approach Bal^[22] and coworker demonstrated the conversion of aniline to azoxybenzene with H₂O₂ as oxidant, while the work of Grützmacher^[23] and coworker used a Rh(I)-catalyst for transfer hydrogenation with alcohols and nitrosobenzene as hydrogen acceptor to form aldehydes and also to generate azoxybenzene. Another work done by Chuang and coworker used isopropanol both as reducing agent and as solvent.^[24] More recently, Fujii and Mori reported the synthesis of azoxybenzenes from nitrobenzenes by light irradiation under continuous flow conditions.^[25] Oppositely, azoxybenzenes were formed as a byproduct in the asymmetric desymmetrization of prochiral ketones to optically active α -hydroxy-ketones.^[26]

Difficulties in these approaches lie in the harsh reaction conditions, over-reduction or oxidation of the educts, and in competition reactions, which include in particular the condensation of anilines with nitrosoarenes to generate diazo compounds.^[17,27] Consequently, there is a great interest in efficient and simplified synthetic strategies for the selective preparation of these valuable compounds, and herein a syn-



Scheme 1. Formation pathways of azoxybenzene.

thesis of azoxybenzenes within minutes at mild reaction conditions is reported.

With the implementation of the MFR concept for the reductive dimerization of nitrosobenzene using an excess of ketone in DMSO and catalytic amounts of proline-polymer-network various nitrosobenzenes were converted to the corresponding azoxybenzene as the major product.

Results and Discussion

For the recent study a gel composition comparable to that used to study the Knoevenagel reaction within a microfluidic reactor was used, with methacrylates as gel-forming compound and using a proline-based catalyst.^[11]

To establish the catalytic behavior of the supported proline, differently composed polymer networks were prepared, immobilizing a proline-based catalyst structure.^[28] First, mono-2-(methacryloyloxy)ethyl succinate was converted into the acid chloride by treatment with thionylchloride. This acid chloride was treated with *trans*-4-hydroxy-L-proline in TFA to generate proline ester derivative **3**. Ester **3** was immobilized via copolymerization with MMA and EGDMA to form a polymer network (Figure 2). To ensure a stable connection of the gel to the surface of the reactor, the object slides were modified with 3-(trichlorosilyl)propylmethacrylate prior to the photopolymerization. The successful modification was investigated by contact angle measurements as shown in Figure S1.

In the case of continuously operated flow reactors, the geometry of the reactor chamber and thus the volume accessible for reactions are predetermined by the design of the reactor. The reactor used has a height of 140 μ m and a total volume of approximately 100 μ l. A schematic illustration of the reactor setup and the course of the photopolymerization is shown in Figure S2–S4. To adapt the properties of the polymer matrix as best as possible to the requirements within the reactor and to those of the desired reaction, the height of the gels in the dry state and the degree of swelling were examined. The change in height of the surface-bound gels can be calculated on the basis of the swelling tests of the free gels, using the relation from R \ddot{u} he.^[29] These results essentially relate to thin polymer films. In contrast, the group around Dostalek examined the swelling behavior of hydrogel columns which is comparable to that of thin films.^[30] Images of the obtained bulk gels are presented in Figure S5. The height of the attached

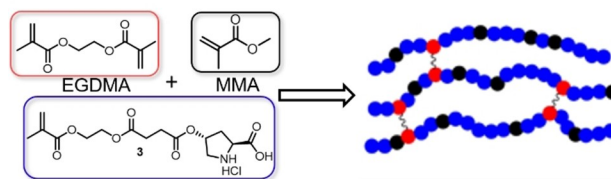


Figure 2. Components of polymergel. Gel building component: methyl methacrylate (MMA), crosslinker: ethylene glycol dimethacrylate (EGDMA), catalyst (**3**)

hexagonally gel-dot structures was determined using confocal microscopy. As can be seen in Figures S6 and S7, the average height was determined to 121 (± 7) μm . As an example, the original data from the confocal microscopy measurements can be seen in Figure S6.

To calculate the height increase of the immobilized gel structures, macroscopic polymer samples with a monomer concentration of 3.34 M, an irradiation time of 12.4 sec, and an intensity of 428 mW with 8 cm distance between sample and light source were prepared. To release the free secondary amine of the proline moiety and to remove the HCl salt, an approach inspired by Tor E. Kristensen was used.^[28,31] This includes washing with methylene chloride followed by washing with mixtures of methanol and triethylamine (9:1) as well as with tetrahydrofuran and triethylamine (9:1) followed by pure tetrahydrofuran and pure methanol as the last purification step. Since the reductive dimerization was performed in DMSO, the degree of swelling was investigated in DMSO as well, which together with proline as catalyst is in good agreement with the requirements of green chemistry.^[7,8] However, since the immobilized polymer structures with crosslinker content <5% did not guarantee sufficient mechanical stability in continuous operation over a long period of time, the polymer composition was fixed at 5% crosslinker, 5% gel building component, and 90% catalyst. This composition of the gel also addresses the well-known problem that organocatalyzed reactions generally require a larger amount of catalyst compared to metal-based catalysts due to their relatively low turnover efficiency.^[32] The degree of swelling in DMSO was investigated for unattached gel samples. In order to transfer results from unattached samples to attached ones, equations S1 and S2 together with swelling results presented in Figure S5 were used.^[29] A degree of swelling of 1.8 was obtained for the above-mentioned polymer composition, which leads to a calculated height extension of 1.38 for attached polymer networks.

With the calculated height extension of attached polymer networks in hands, the polymer height in dry state was used as a basis for the calculation of the height in a swollen state. Since it was already apparent in the first test runs that polymer compositions with crosslinker contents of <5% seemed to not have sufficient mechanical stability, the height of the gel structures was adjusted in such a way that stabilization through the cover of the reactor chamber is also possible by exceeding the 140 μm height of the reactor chamber. Using a polymer composition containing of 90% catalyst, 5% crosslinker, and 5% gel-forming component led to polymers with a calculated height of 166 μm in swollen state and thus exceeds the height of the reactor cell, which leads to more robust polymer-dot arrays. Hence, this composition was selected for further analysis, due to the two major advantages of the polymer composition. On the one hand, an additional stabilizing effect against mechanical deformation was established by exceeding the 140 μm of the reactor cell, on the other hand, the polymer composition showed the most pronounced feedback in terms of conversion in the first test runs using **2a**.

To test the applicability of the selected organic reaction and the integrated catalyst **3**, inside the polymeric network of

surface-attached gels under different conditions, first, the optimization of the reductive dimerization of nitrosoarene **2a** to form azoxyarene **1a** was carried out inside the MFR. As shown in Table 1, different solvents, as well as different additives, were tested in the reaction at room temperature ($\sim 23^\circ\text{C}$).

The reductive dimerization of the unsubstituted nitrosobenzene **2a** was evaluated as model reaction. Following key issues could be validated: Since the solvent is responsible for both the solubility of the educts and products as well as for the swelling of the polymer gel, DMF and DMSO were chosen for further analysis. In DMF and DMSO (entries 1 and 2) no conversion was detected without the additive being present. With 1 eq of cyclohexanone as additive in DMF, 58% conversion was obtained (entry 3). A conversion of 72% after a residence time of 100 min was detected using 1 eq of cyclohexanone in DMSO (entry 4). Under the same reaction conditions using a gel without catalyst no conversion was detected (entry 5). Halving the residence time to 50 min (entry 6) or performing reactions at higher concentrations of **2a** at 0.4 M and the additive at 0.2 M led to a decreased conversion (entry 8), possibly the generally low turnover number for organocatalysts.^[33] Using other ketones such as acetone (entry 7) as an additive, only traces of the desired product were obtained. This finding can possibly be attributed to a faster condensation kinetic and the ability of cyclohexanone to act as an excellent donor compared with acetone.^[34]

To produce larger quantities of product, a gel-bound organocatalyst is required to have outstanding stability and reusability. As shown in Figure 3, the conversion of **2a** only slightly decreases with a longer reaction time. Specifically, after almost 24 h of reaction time 91 (± 11) % conversion can be retained, when the flow rate is kept at $1.0 \mu\text{L min}^{-1}$ (see Figure S8). The running time was further extended to five days, applying a flow rate of $2.0 \mu\text{L min}^{-1}$ (see Figure S9). Even after five days, a conversion of still 67 (± 9) % was observed. The decrease in conversion of **2b** can be explained by two different

Table 1. Optimization of Reaction Conditions.

Entry	Solvent	Additive	Conversion [%] ^[a]
1	DMF	–	–
2	DMSO	–	–
3	DMF	Cyclohexanone	58
4	DMSO	Cyclohexanone	72
5 ^[b]	DMSO	Cyclohexanone	–
6 ^[c]	DMSO	Cyclohexanone	56
7	DMSO	Acetone	traces
8 ^[d]	DMSO	Cyclohexanone	43

[a] Determined by $^1\text{H-NMR}$. [b] Conversion of reference sample under the same reaction conditions using a gel without catalyst. Determined from $^1\text{H-NMR}$ of crude product. [c] Dwell time of 50 min. [d] Reaction of 0.4 M of starting material respective 0.2 M additive.

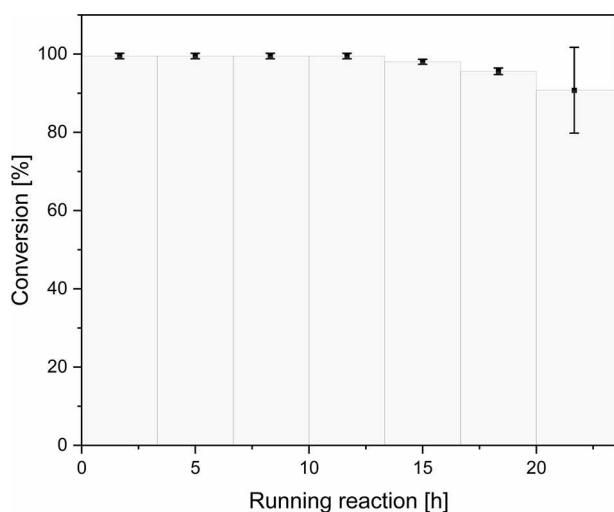


Figure 3. Long-term conversion behavior of the MFR measured by NMR when 4-nitrosobenzonitrile is injected at $1.0 \mu\text{L min}^{-1}$ the reaction time is 100 min.

factors. The first factor is the inactivation of the catalyst due to repeated uses over time. The second factor is a possible enrichment of reactant as well as of azoxybenzene-molecules inside the gel dots due to undesired non-covalent interactions. This hypothesis would correspond to the observable color change of the gel dots shown in Figure 4 as an example. Figure 4 shows the gradual color change of the gel dots from the reactor inlet to the reactor outlet. The intensity of the coloring of the polymer dots decreased along the direction of flow of the reactant solution within the MFR. This could indicate a progressive accumulation of product within the gel dots. For the synthesis of 1,2-bis(4-cyanophenyl)diazene oxide (**1b**) from 4-nitrosobenzonitrile (**2b**) with cyclohexanone as an additive, the educt solution has a light green color, whereas a sample of the product solution collected over 24 h has an intense yellowish color (Figure 4).

Based on the good long-term stability, a wide variety of differently substituted nitrosobenzenes was subjected to the reaction conditions, the results are shown in Table 2. The reductive dimerization of nitrosoarenes yielding azoxybenzenes

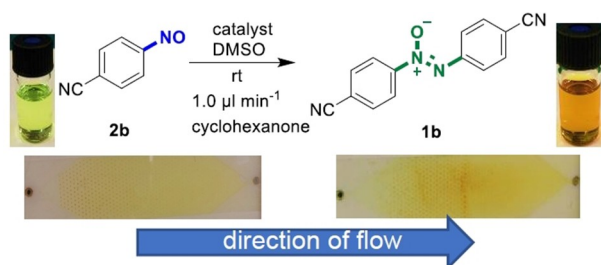


Figure 4. Color change of the MFR from light yellow after 1 h on the left to intense yellow after 24 h on the right, when 4-nitrosobenzonitrile is injected at $1.0 \mu\text{L min}^{-1}$. Educt solution on the left, typical product solution on the right.

Table 2. Substrate scope of reductive dimerization of nitrosobenzenes in continuous flow.^[a]

$2.0 \text{ eq. } \text{R-C}_6\text{H}_4\text{-NO} + 1.0 \text{ eq. additive} \xrightarrow[\text{50-200 min}]{\text{catalyst, solvent, rt}}$ $\text{R-C}_6\text{H}_4\text{-N}^+\text{=N}^-\text{-C}_6\text{H}_4\text{-R}$		
 1b 99% ^[b] (50 min), ^[c] 98% ^[d]	 1c 98% ^[b] (50 min), ^[c] 93% ^[d]	 1d 98% ^[b] (50 min), ^[c] 86% ^[d]
 1e 99% ^[b] (50 min), ^[c] 82% ^[d]	 1f 98% ^[b] (50 min), ^[c] 66% ^[d]	 1g 98% ^[b] (50 min), ^[c] 67% ^[d]
 1h 93% ^[b] (50 min), ^[c] 68% ^[d]	 1i 93% ^[b] (50 min), ^[c] 74% ^[d]	 1j 95% ^[b] (50 min), ^[c] 72% ^[d]
 1k 84% ^[b] (50 min), ^[c] 61% ^[d]	 1a 72% ^[b] (100 min), ^[c] 61% ^[d]	 1l 58% ^[b] (200 min), ^[c] 52% ^[d]
 1m 91% ^[b] (200 min), ^[c] 73% ^[d]	 1n 0% ^[b] , ^[b,e] (200 min), ^[c] 0% ^[d]	

[a] Reaction of 0.05 M of starting material. [b] Conversion determined from ¹H-NMR of crude product [c] Dwell time inside the reactor [d] Isolated yield [e] Starting material recovered.

could be applied to a wide scope of differently substituted nitrosobenzenes. The reactions were studied with two equivalents of nitrosobenzene and one equivalent of cyclohexanone as additive. Regardless of the nature and position of the substituents at the ring, the conversions and yields being good to excellent, ranging from 58% to 99% and 52% to 99% respectively. It was observed that in cases of electron-donating substituents such as alkyl groups, the reaction times to reach high conversions were longer compared to electron-withdrawing ones such as halides, esters, and cyanides. Nitrosobenzenes with electron-withdrawing groups such as cyano (**2b**, and **2j**), nitro (**2c**), and ester (**2d**, **2h**) at different positions were converted to the corresponding products in 93–99%, respective 68–98% isolated yields. Reactions of halogen-substituted nitrosobenzenes (**2f**, **2g**, **2i**, and **2k**) led to conversions of 84–98% and isolated yields of 66–74%. Furthermore, reactions of unsubstituted nitrosobenzene (**2a**) and reactions with electron-donating groups of alkyl (**2l**, **2m**) at different positions were found to give lower conversions and required a longer reaction

time with conversions from 58–91 % and isolated yields ranging from 52–73 %. A possible origin of the observed differences between conversion and yield could be enrichment processes of different degrees, in particular of the dipolar product molecules into the gel matrix. In the case of the *p*-dimethylamino group (**2n**), only starting material was recovered. This is attributable to the electron abundance of the benzene moiety due to the particularly pronounced plus-I effect of the *p*-dimethylamino substituent and the resulting low formation of the dimer structure.^[35,36] An evaluation of the reactions mentioned above indicates that both substituents in *ortho* position and electron-donating substituents inhibit the conversion of the nitroso compounds into the corresponding azoxy compounds, which is in agreement with results reported in the literature.^[24] One of the isolated products, **1f**, was characterized by single-crystal X-ray diffraction as shown in Figure 5. The single-crystal X-ray structure obtained proves the exclusive formation of trans adducts.

In addition to the production of “symmetrical” azoxy compounds, the examination of the MFR-concept for the synthesis of “asymmetric” adducts was also of interest (Scheme 2). In principle, the mixing of two differently substituted nitrosobenzenes should result in four different azoxy compounds after the reaction.

After a reaction of **2d** with **2g** and **2c** with **2h**, almost exclusively symmetrical adducts of both nitroso compounds were detected in the reaction mixture. Compounds **1dg** and **1ch** were detected in traces in the reaction mixture only. This is in line with the results of Chuang,^[24] where symmetrical azoxybenzenes were also obtained as the dominant product species. In the case of the MFR concept, this tendency seems to be reinforced, possibly by the different concentrations of

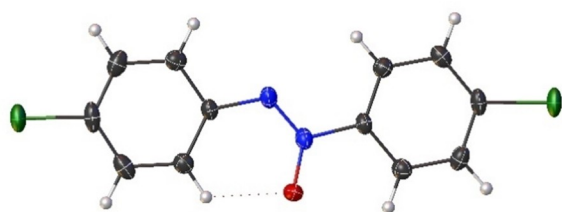
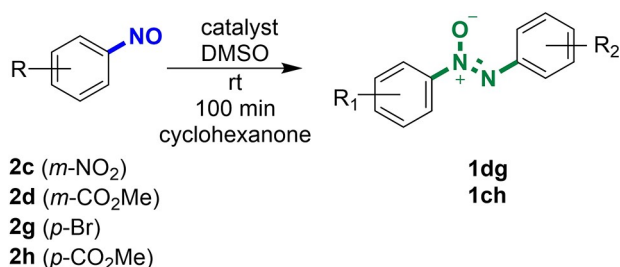


Figure 5. ORTEP diagram of **1f**.



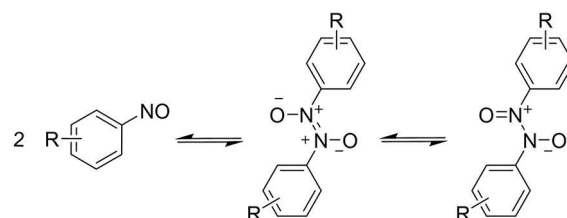
Scheme 2. Overview reaction for the synthesis of asymmetric adducts. In both reactions, small amounts of starting materials were recovered.

reactants and the low reaction temperature which does not lead to the formation of mixed dimers.

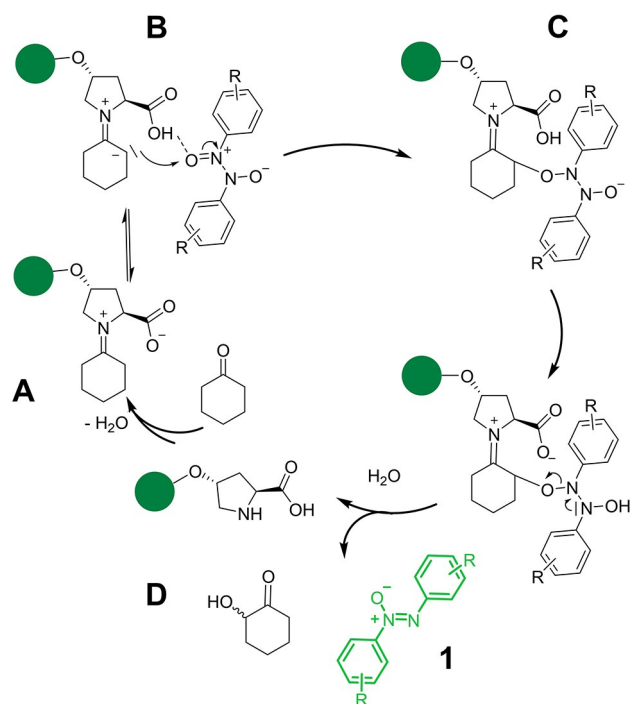
The improved reactivity of electron-poor nitroso compounds and the identification of hydroxycyclohexanone in the reaction solution indicate a possible reaction mechanism. As can be seen in Figure S10, the characteristic ¹H-NMR-signals as described previously^[26] as well as a detailed analysis of the coupling of the hydroxy group and the proton in alpha position to the carbonyl function in hydroxycyclohexanone via 1D selective gradient COSY spectra are shown in the Figures S11–S13. Nitrosobenzenes are well known to form dimers in a reversible equilibrium.^[35] Nitrosobenzenes carrying electron-withdrawing substituents tend to favor the formation of dimers.^[35] A key to a possible mechanism is the presence of the dimer structures, as shown in scheme 3. In the MFR a relative high concentration of nitrosobenzenes were used^[26,36,37] favoring dimer formation in conjunction with longer periods of rest in the syringe within the syringe pump. Further, no or only very little α -aminoxy ketone^[37] and no formation of asymmetric azoxybenzenes were detected.

As shown in Scheme 4a possible mechanism for the formation of azoxybenzenes from nitrosobenzenes is proposed. The mechanism can be seen as a supplement to the work of Barbas and colleagues, who were able to produce α -hydroxyketones using L-proline, cyclic ketones, and nitrosobenzene.^[26] First, the secondary amine and the keto-species condense under the formation of an iminium ion **A**. This is followed by a nucleophilic attack of the condensation product to the oxygen attached to a cationic nitrogen of the dimer (**B**), which forms intermediate **C**. Besides this, nucleophilic addition of the condensation product to excess nitrosobenzene may also take place, furnishing the α -aminoxy ketone.^[26] Addition to excess nitrosoarene again leads to intermediate **C**.^[21] However, as stated above this seems not to be favorable. Tautomerization and hydrolysis of **C** leads to the formation of the trans-azoxyarene **1** and hydroxycyclohexanone **D**. Spectroscopic analyzes which, however, also indicate that further reaction paths being taken, support the formation of α -hydroxycyclohexanone. In this context, in particular, the poorer results for acetone appear to be reasonable.^[34]

The turnover frequency (TOF) and turnover number (TON) were calculated to enable a comparison of our synthetic approach with other systems. The results are summarized in Table 3. In the case of the MFR approach, TON between 3.34 and 1.27 and TOF values ranging from 3.02 h⁻¹ to 0.31 h⁻¹ were



Scheme 3. Equilibrium between monomer and dimer structures of nitrosobenzenes.



Scheme 4. Proposed mechanism for the reductive dimerization of nitrosoarenes forming azoxyarenes using an immobilized proline catalyst.

Table 3. Calculated TON and TOF for different reactions. $2.41 \cdot 10^{-2}$ mmol of catalyst (immobilized on surface) and a 0.05 M reactant solution were used. The conversions and reaction running times were used for TON calculations, isolated yields and dwell times of the MFR were used for TOF calculations.

Nitrosobenzene [l]	Reaction running time [h]	TON [l]	Dwell time [min]	TOF [h ⁻¹]
2b	23	2.53	50	3.02
2c	18	1.97	50	2.25
2d	17.7	1.92	50	2.07
2e	21.5	2.22	50	2.21
2f	17	1.82	50	2.25
2g	24	2.02	50	2.52
2h	16	1.64	50	1.43
2i	22	2.23	50	2.10
2j	17	3.34	50	3.02
2k	22	2.02	50	0.91
2a	20	1.49	100	0.31
2l	21	1.27	200	0.33
2m	44	2.49	200	0.54

obtained. In contrast to that, mainly metal-based catalysts were described for the synthesis of azoxyarenes under batch conditions with TON between 8 and 32 and TOF between 0.5 h^{-1} and 2 h^{-1} .^[38] Although a comparison of different TON and TOF is hardly possible due to the many influencing parameters, the results obtained for the MFR system are within the range of systems described in literature.^[38] Nevertheless, higher TON and TOF values for the synthesis of azoxyarenes from different starting materials can be achieved using metal catalysts under batch conditions.^[39] In spite of this, in comparison to the presented MFR approach, higher temperatures or significantly longer reaction times in combination with other

harsh additives, such as H_2O_2 are required for the synthesis of azoxy compounds in all of the cases mentioned. To the best of our knowledge, the results outlined in this work represent the first synthesis sequence of azoxybenzenes, starting from nitroso compounds within a microfluidic reactor using gel-bound catalysts at room temperature within minutes of residence time.

Conclusion

As conclusion, the properties of a proline-carrying polymer network were successfully adjusted in order to develop a versatile synthesis approach for the production of azoxybenzenes from nitrosobenzenes. Gel-bound proline serves as a catalyst and cyclohexanone as an additive for this reductive dimerization. The properties of the methacrylate-based gel were adjusted in such a way that they enabled sufficient swelling, but at the same time could withstand the mechanical stresses of continuous operation. With the optimized parameters in hand, the MFR was successfully used for the synthesis of a wide range of differently substituted azoxybenzenes. The different tendencies of nitroso compounds to form dimer structures and their influence on reaction time, conversion and yield were in agreement with previous findings.^[24] Apart from that, the established MFR also presents a good long-term activity for the continuous production of azoxybenzenes over 24 and 120 hours, respectively.

Experimental Section

The monomer methyl methacrylate (99%) (MMA) and the cross-linker ethylene glycol dimethacrylate (98%) (EGDMA) were purchased from *Tokyo Chemical Industries (TCI)*. Mono-2 (methacryloyloxy)ethyl succinate (95 + %) was purchased from *Sigma Aldrich*. *Trans-4-hydroxy-L-proline* (>99%) was purchased from *TCI*. Tri-fluoroacetic acid (>99%) was purchased from *Carl Roth*. The reactants for initiator synthesis, dimethylphenylphosphonite (98%) was purchased from *Sigma-Aldrich*, while 2,4,6-trimethylbenzoylchloride (98 + %) and 2-butanone (99%) were purchased from *Alfa Aesar*. 3-(Trichlorosilyl)propylmethacrylate (>90%) was used for surface modification and was purchased from *Sigma-Aldrich*. Cyclohexanone (99.8%) was purchased from *Acros Organics*. The solvents used for the surface modification as well as for the workup of the polymer-dots: isopropanol, ethanol, methanol, tetrahydrofuran (THF), and dichloromethane (DCM) were technical grade and purchased from local suppliers. Triethylamine ($\geq 99.5\%$) was purchased from *Sigma Aldrich*. For flow experiments, dimethyl sulfoxide (DMSO) analytical grade was purchased from *Grüssing GmbH*.

Analysis methods

Confocal Microscopy The confocal microscope Keyence "VK-9700" was used for height determination of polymer dots. Images were taken with the software "VK Viewer 2.4.0.1" and the analysis of polymer height was done with the software "VK Analyzer 3.4.0.1".

Nuclear magnetic resonance spectroscopy The $^1\text{H-NMR}$ spectra for conversion determination were measured on a Bruker "Ascent 700" spectrometer. Product spectra of synthesized products were measured on a Bruker "Avance 500" (^1H , 500.1 MHz; ^{13}C , 125.8 MHz;

³¹P, 202.0 MHz) and "Ascent 700" (¹H, 700.1 MHz; ¹³C, 176.0 MHz) spectrometer, using different solvents purchased by Deutero. The NMR signals were referenced to residual solvents measured relative to TMS as internal standard.

Electron impact mass spectrometry The EI-MS measurements were done with a high-resolution sector field "DFS" mass spectrometer from Thermo scientific.

Electrospray ionization mass spectrometry The ESI-MS measurements were done with a "Synapt-G2 HDMS" mass spectrometer from Waters. The spectrometer is used in combination with a time-of-flight analyzer.

Contact angle measurement The contact angle measurements were performed using a "Drop Shape Analyzer-DSA25" from Krüss. Using Diiodomethane ReagentPlus (99%) from Sigma-Aldrich and Water Rotisolvl HPLC Gradient Grade from Roth.

Melting points The melting points were determined on a Melting Point B-545 (Büchi). A gradient of 1 °C/min was applied.

General Procedure for the Reductive Dimerization of Nitrosobenzenes, 2 To Form Azoxybenzenes 1

A solution of **2** in DMSO (0.05 M; 2 eq) with cyclohexanone (1 eq) in a Hamilton™ 1000 Series Gastight™ Syringe was injected via a Legato 200 syringe pump into the MFR. After 16–44 h of running reaction and quenching of the crude product solution using sat. NH₄Cl solution, the reaction mixture was extracted using DCM or EtOAc. After phase separation, the solvent was evaporated by rotavap, and **1** was isolated using column chromatography of the crude product.

General Procedure for the Reductive Dimerization of Nitrosobenzenes, 2 To Form unsymmetric Azoxybenzenes 1

Two separate solutions of the nitroso compound in DMSO (0.05 M; 2 eq) with cyclohexanone (1 eq) in a Hamilton™ 1000 Series Gastight™ Syringe were injected into the MFR via two syringes using a T-junction using a Legato 200 syringe. After 24 h of running reaction and quenching of the crude product solution using sat. NH₄Cl solution, the reaction mixture was extracted using DCM or EtOAc. After phase separation, the solvent was evaporated by rotavap.

The differently substituted nitrosobenzenes used were prepared by the oxidation of the corresponding aniline derivatives using oxone as described by Rück-Braun and coworker.^[40]

1,2-Bis(4-cyanophenyl)diazene oxide 1b (15 mg, 98%; yellowish solid, mp = 195.7–198.1 °C): R_f = 0.13 (EtOAc/n-hexane = 1:8); ¹H NMR (700 MHz, CDCl₃, 24 °C, δ): 8.46 (d, J = 8.5 Hz, 2H), 8.23 (d, J = 8.5 Hz, 2H), 7.87 (d, J = 8.9 Hz, 2H), 7.79 (d, J = 8.7 Hz, 2H). ¹³C NMR (176 MHz, CDCl₃, 24 °C, δ): 150.6 (C), 146.7 (C), 133.5 (CH×2), 133.2 (CH×2), 126.4 (CH×2), 123.7 (CH×2), 118.6 (C), 117.7 (C), 116.5 (C), 113.5 (C). LRMS (EI-TOF): m/z calculated for C₁₄H₈N₄O [M]⁺, 248.0698; found, 248.0425.

1,2-Bis(3-nitrophenyl)diazene oxide 1c (13 mg, 93%, white solid, mp = 145.3 – 146.4 °C): R_f = 0.15 (EtOAc/n-hexane = 1:6); ¹H NMR (700 MHz, CDCl₃, 24 °C, δ): 9.21 (t, J = 2.0 Hz, 1 H), 9.12 (t, J = 2.0 Hz, 1 H), 8.71 (ddd, J = 8.2, 2.1, 0.9 Hz, 1 H), 8.49 (m, 2 H), 8.31 (ddd, J = 8.2, 2.1, 0.9 Hz, 1 H), 7.79 (t, J = 8.3 Hz, 1 H), 7.71 (t, J = 8.2 Hz, 1 H). ¹³C NMR (176 MHz, CDCl₃, 24 °C, δ): 148.5 (C), 148.4 (C×2), 143.9 (C), 131.6 (CH), 130.3 (CH), 129.8 (CH), 128.0 (CH), 126.8 (CH), 124.6 (CH), 120.5 (CH), 118.1 (CH). LRMS (EI-TOF): m/z calculated for C₁₂H₈N₄O₅ [M]⁺, 288.0495; found, 288.0316.

Dimethyl 3,3'-diazene oxide 1,2-diylidbenzoate 1d (13 mg, 86%, yellow solid, mp = 134.2–136.6 °C): R_f = 0.46 (CH₂Cl₂) (CH₂Cl₂/n-pentane = 1:3); ¹H NMR (700 MHz, CDCl₃, 24 °C, δ): 8.97 (t, J = 1.8 Hz, 1 H), 8.78 (t, J = 1.7 Hz, 1 H), 8.53 (ddd, J = 8.2, 2.3, 1.1 Hz, 1 H), 8.43 (ddd, J = 8.1, 2.0, 1.2 Hz, 1 H), 8.26 (ddd, J = 7.8, 1.3, 1.3 Hz, 1 H), 8.09 (ddd, J = 7.8, 1.4, 1.4 Hz, 1 H), 7.63 (t, J = 7.9 Hz, 1 H), 7.58 (t, J = 8.9 Hz, 1 H), 3.99 (s, 3 H), 3.96 (s, 3 H). ¹³C NMR (176 MHz, CDCl₃, 24 °C, δ): 166.5 (C), 165.7 (C), 148.3 (CH), 143.8 (C), 132.8 (CH), 131.4 (CH), 130.9 (CH), 130.7 (CH), 129.4 (CH), 129.1 (CH), 128.9 (CH), 127.1 (CH), 126.5 (CH), 123.6 (CH), 52.6 (CH₃), 52.4 (CH₃). LRMS (EI-TOF): m/z calculated for C₁₆H₁₄N₂O₅ [M]⁺, 314.0903; found, 314.0493.

1,2-Bis(3-cyanophenyl)diazene oxide 1e (11 mg, 82%, pale yellow solid, mp = 133.1–134.3 °C): R_f = 0.08 (EtOAc/n-hexane = 1:8); ¹H NMR (700 MHz, CDCl₃, 24 °C, δ): 8.65 (t, J = 1.8, 1 H), 8.60–8.57 (m, 2 H), 8.32 (ddd, J = 8.2, 1.7 Hz, 1.3 Hz, 1H), 7.91–7.89 (dt, J = 1.5, 1.5 Hz, 1H), 7.73–7.69 (m, 2H), 7.65–7.61 (m, 1H). ¹³C NMR (176 MHz, CDCl₃, 24 °C, δ): 148.3 (C), 143.9 (C), 135.6 (CH), 133.4 (CH), 130.42 (CH), 130.41 (CH), 130.1 (CH), 129.1 (CH), 126.8 (CH), 126.5 (CH), 118.2 (C), 117.4 (C), 113.8 (C), 113.5 (C). LRMS (EI-TOF): m/z calculated for C₁₄H₈N₄O [M]⁺, 248.0698; found, 248.0501.

1,2-Bis(4-chlorophenyl)diazene oxide 1f (8 mg, 66%, pale yellow solid, mp = 152.0–154.1 °C): R_f = 0.25 (EtOAc/n-hexane = 1:50); ¹H NMR (700 MHz, CDCl₃, 24 °C, δ): 8.25 (d, J = 9.1 Hz, 2H), 8.16 (d, J = 9.0 Hz, 2H), 7.49 (d, J = 9.1 Hz, 2H), 7.45 (d, J = 9.0 Hz, 2H). ¹³C NMR (176 MHz, CDCl₃, 24 °C, δ): 146.6 (C), 142.3 (C), 138.1 (C), 135.3 (C), 129.1 (CH×2), 129.0 (CH×2), 127.1 (CH×2), 123.7 (CH×2). LRMS (EI-TOF): m/z calculated for C₁₂H₈Cl₂N₂O [M]⁺, 266.0014; found, 265.9744.

1,2-Bis(4-bromophenyl)diazene oxide 1g (12 mg, 67%, yellowish solid, mp = 166.5–168.4 °C): R_f = 0.25 (EtOAc/n-hexane = 1:8); ¹H NMR (700 MHz, CDCl₃, 24 °C, δ): 8.18 (d, J = 8.9 Hz, 2H), 8.08 (d, J = 8.8 Hz, 2H), 7.65 (d, J = 8.9 Hz, 2H), 7.61 (d, J = 8.8 Hz, 2H). ¹³C NMR (176 MHz, CDCl₃, 24 °C, δ): 147.1 (C), 142.6 (C), 132.1 (CH×2), 132.0 (CH×2), 127.3 (CH×2), 126.5 (C), 123.9 (CH×2), 123.6 (C). LRMS (EI-TOF): m/z calculated for C₁₂H₈Br₂N₂O [M]⁺, 355.8983; found, 355.8945.

Dimethyl 4,4'-diazene oxide 1,2-diylidbenzoate 1h (9 mg, 68%, yellow solid, mp = 199.1–201.4 °C): R_f = 0.39 (CH₂Cl₂) (CH₂Cl₂/n-hexane = 1:3); ¹H NMR (700 MHz, CDCl₃, 24 °C, δ): 8.39 (d, J = 8.6 Hz, 2H), 8.22–8.15 (m, 6H), 3.97 (s, 3H), 3.95 (s, 3H). ¹³C NMR (176 MHz, CDCl₃, 24 °C, δ): 166.2 (C), 165.8 (C), 150.9 (C), 147.0 (C), 133.3 (C), 130.7 (C), 130.4 (CH×2), 130.2 (CH×2), 125.4 (CH×2), 122.6 (CH×2), 52.6 (CH₃), 52.3 (CH₃). LRMS (EI-TOF): m/z calculated for C₁₆H₁₄N₂O₅ [M]⁺, 314.0903; found, 314.0557.

1,2-Bis(3-bromophenyl)diazene oxide 1i (15 mg, 74%, yellowish solid, mp = 107.5–109.8 °C): R_f = 0.5 (EtOAc/n-hexane = 1:7); ¹H NMR (700 MHz, CDCl₃, 24 °C, δ): 8.47 (t, J = 1.9 Hz, 1 H), 8.41 (t, J = 1.9 Hz, 1 H), 8.26–8.23 (m, 1H), 8.07–8.04 (m, 1 H), 7.73–7.69 (m, 1 H), 7.56–7.53 (m, 1 H), 7.40 (t, J = 8.2 Hz, 1 H), 7.37 (t, J = 8.1 Hz, 1 H). ¹³C NMR (176 MHz, CDCl₃, 24 °C, δ): 149.2 (C), 145.1 (C), 135.3 (CH), 133.2 (CH), 130.6 (CH), 130.4 (CH), 128.7 (CH), 126.1 (CH), 124.9 (CH), 122.9 (C), 122.7 (C), 121.5 (CH). LRMS (EI-TOF): m/z calculated for C₁₂H₈Br₂N₂O [M]⁺, 355.8983; found, 355.8794.

1,2-Bis(2-cyanophenyl)diazene oxide 1j (15 mg, 72%, yellowish solid, mp = 192.4–193.5 °C): R_f = 0.16 (EtOAc/n-hexane = 1:8); ¹H NMR (700 MHz, CDCl₃, 24 °C, δ): 8.87 (d, J = 8.1 Hz, 1 H), 8.47 (d, J = 8.3 Hz, 1 H), 7.91 (dd, J = 7.5, 1.4 Hz, 1H), 7.85–7.77 (m, 2H), 7.76–7.70 (m, 2H), 7.53 (t, J = 7.6 Hz, 1H). ¹³C NMR (176 MHz, CDCl₃, 24 °C, δ): 149.4 (C), 144.9 (C), 135.6 (CH), 134.1 (CH), 133.9 (CH), 133.7 (CH), 132.5 (CH), 130.6 (CH), 125.3 (CH), 123.7 (CH), 116.8 (C), 116.1 (C), 111.9 (C), 108.1 (C). LRMS (EI-TOF): m/z calculated for C₁₄H₈N₄O [M]⁺, 248.0698; found, 248.0627.

1,2-Bis(2-bromophenyl)diazene oxide 1k (13 mg, 61%, orange solid, mp = 108.2–112.5 °C): R_f = 0.16 (EtOAc/n-hexane = 1:5); ^1H NMR (700 MHz, CDCl_3 , 24 °C, δ): 7.97 (dd, J = 8.0, 1.5 Hz, 1 H), 7.77–7.70 (m, 3 H), 7.51–7.35 (m, 3 H), 7.23–7.20 (m, 1 H). ^{13}C NMR (176 MHz, CDCl_3 , 24 °C, δ): 149.2 (C), 142.4 (C), 134.3 (CH), 133.6 (CH), 131.5 (CH), 129.9 (CH), 128.4 (CH), 127.9 (CH), 125.4 (CH), 123.6 (CH), 119.5 (C), 115.2 (C). LRMS (EI-TOF): m/z calculated for $\text{C}_{12}\text{H}_8\text{Br}_2\text{N}_2\text{O}$ $[\text{M}]^+$, 355.8983; found, 355.8829.

1,2-Diphenyldiazene oxide 1a (5 mg, 61%, yellowish solid, mp < 35 °C): R_f = 0.38 (EtOAc/n-hexane = 1:50); ^1H NMR (700 MHz, DMSO, 24 °C, δ): 8.26 (m, 2H), 8.08 (m, 2H), 7.78–7.72 (m, 1H), 7.66–7.62 (m, 2H), 7.58–7.54 (m, 2H), 7.49–7.45 (m, 1H). ^{13}C NMR (176 MHz, CDCl_3 , 24 °C, δ): 148.4 (C), 144.0 (C), 131.5 (CH \times 2), 129.6 (CH \times 2), 128.8 (CH \times 2), 128.7 (CH \times 2), 125.5 (C), 122.3 (C). LRMS (EI-TOF): m/z calculated for $\text{C}_{12}\text{H}_{10}\text{N}_2\text{O}$ $[\text{M}]^+$, 198.0793; found, 198.0907.

1,2-Di-*o*-tolylidiazene oxide 1l (6 mg, 52%, yellowish solid, mp = 57.8–58.5 °C): R_f = 0.25 (EtOAc/n-hexane = 1:30); ^1H NMR (700 MHz, CDCl_3 , 24 °C, δ): 8.03 (d, J = 8.1 Hz, 1H), 7.70–7.66 (m, 1H), 7.42–7.36 (m, 1H), 7.36–7.23 (m, 6 H), 2.52 (s, 3H), 2.37 (s, 3H). ^{13}C NMR (176 MHz, CDCl_3 , 24 °C, δ): 149.7 (C), 142.9 (C), 134.3 (C), 131.9 (CH), 131.4 (C), 130.9 (CH), 130.2 (CH), 128.8 (CH), 126.8 (CH), 126.2 (CH), 123.8 (CH), 121.7 (CH), 18.7 (CH), 18.6 (CH). LRMS (ESI-TOF (pos.)): m/z calculated for $\text{C}_{14}\text{H}_{14}\text{N}_2\text{O}$ $[\text{M}]^+$, 226.1106; found, 227.1174.

1,2-Bis(4-ethylphenyl)diazene oxide 1m (11 mg, 73%, yellowish oil): R_f = 0.16 (EtOAc/n-hexane = 1:120); ^1H NMR (700 MHz, CDCl_3 , 24 °C, δ): 8.21 (d, J = 8.5 Hz, 2H), 8.14 (d, J = 8.4 Hz, 2H), 7.35–7.29 (m, 4H), 2.78–2.68 (m, 4H), 1.32–1.24 (m, 6H). ^{13}C NMR (176 MHz, CDCl_3 , 24 °C, δ): 148.3 (C), 146.6 (C), 146.4 (C), 142.2 (C), 128.8 (CH), 128.7 (CH), 128.3 (CH), 128.2 (CH), 125.9 (CH \times 2), 122.4 (CH \times 2), 29.1 (CH_2), 28.8 (CH_2), 15.6 (CH_3), 15.5 (CH_3). LRMS (EI-TOF): m/z calculated for $\text{C}_{16}\text{H}_{18}\text{N}_2\text{O}$ $[\text{M}]^+$, 254.1419; found, 254.1343.

Initiator used for polymerization: Lithium phenyl-2,4,6-trimethylbenzoylphosphinate (LAP)^[11,41] (1.76 g, 65%; colorless solid)

^1H NMR (500 MHz, D_2O , 24 °C, δ): 7.73 (dd, J = 7.3 Hz; J = 11.4 Hz, 2H), 7.49 (t, J = 7.8 Hz, 1H), 7.42 (dt, J = 7.7 Hz, J = 3.1 Hz, 2H), 6.80 (s, 2H), 2.16 (s, 3H), 2.01 (s, 6H). ^{13}C NMR (125 MHz, D_2O , 24 °C, δ): 238.8 (C), 138.3 (C), 138.0 (C), 133.7 (C), 133.5 (C), 132.5 (C), 132.3/132.4 (CH), 132.1 (CH), 128.4/128.5 (CH), 128.1 (CH), 20.3 (CH_3), 18.5 (CH_3). ^{31}P -NMR (202 MHz, D_2O , 24 °C, δ): 12.31 (s).

LRMS (ESI-MS): m/z calculated for $\text{C}_{16}\text{O}_3\text{PH}_{16}\text{Na}$ $[\text{M}]^+$, 311.0808; found, 311.0795

Immobilized catalyst structure: O-(2-Methacryloyloxyethylsuccinoyl)-trans-4-hydroxy-L-prolin (MAOESLP)^[27] (10.78 g, 72%, colorless solid, mp = 81–84 °C) ^1H NMR (500 MHz, DMSO- D_6 , 24 °C, δ): 10.32 (s, 1H, br), 9.06 (s, 1H, br), 6.03 (d, J = 1.6 Hz, 1H), 5.70 (d, J = 1.6 Hz, 1H), 5.24–5.35 (m, 1H), 4.39–4.45 (m, 1H), 4.25–4.30 (m, 1H), 3.49–3.66 (m, 1H), 3.21–3.29 (m, 1H), 2.54–2.68 (m, 4H), 2.36–2.40 (m, 1H), 2.27–2.33 (m, 1H), 1.88 (s, 3H). ^{13}C NMR (125 MHz, DMSO- D_6 , 24 °C, δ): 173.03 (C), 171.65 (C), 171.07 (C), 169.24 (C), 166.19 (C), 135.40 (C), 125.93 (CH), 72.22 (CH), 62.16 (CH), 61.85 (CH), 57.38 (CH), 45.22 (CH), 33.83 (CH), 28.51 (CH), 28.19 (CH), 17.69 (CH $_3$). LRMS (ESI-MS): m/z calculated for $\text{C}_{15}\text{O}_8\text{NH}_{21}$ $^+$, 343.1257 found, 342.1214.

Supporting information

(see footnote on the first page of this article): Materials information, experiment, the spectral data of title compounds, and the NMR spectra of products and detailed crystallographic data for 1f. Deposition Number 2038674 (for 1f) contains the supplementary crystallographic data for this paper. These data are provided free of charge by the joint Cambridge Crystallographic Data Centre and Fachinformationszentrum Karlsruhe Access Structures service www.ccdc.cam.ac.uk/structures.

Acknowledgements

The *Kunststofftechnik Paderborn (KTP)* is acknowledged for the Confocal Laser Microscope. Open access funding enabled and organized by Projekt DEAL.

Conflict of Interest

The authors declare no conflict of interest.

Keywords: Continuous flow · Gel-bound catalysts · Microfluidic reactor · Organocatalysis · Synthetic methods

- [1] G. Jas, A. Kirschning, *Chem. Eur. J.* **2003**, *9*, 5708.
- [2] C. J. Welch, X. Gong, J. Cuff, S. Dolman, J. Nyrop, F. Lin, H. Rogers, *Org. Process Res. Dev.* **2009**, *13*, 1022.
- [3] D. C. Fabry, E. Sugiono, M. Rueping, *React. Chem. Eng.* **2016**, *1*, 129.
- [4] S. K. Kurt, M. G. Gelhausen, N. Kockmann, *Chem. Eng. Technol.* **2015**, *38*, 1122.
- [5] a) M. O'Brien, I. R. Baxendale, S. V. Ley, *Org. Lett.* **2010**, *12*, 1596; b) C. B. McPake, C. B. Murray, G. Sandford, *Tetrahedron Lett.* **2009**, *50*, 1674.
- [6] M. Movsisyan, E. I. P. Delbeke, J. K. E. T. Berton, C. Battilocchio, S. V. Ley, C. V. Stevens, *Chem. Soc. Rev.* **2016**, *45*, 4892.
- [7] J. H. Clark, *Green Chem.* **1999**, *1*, 1.
- [8] P. T. Anastas, J. C. Warner, *Green chemistry. Theory and practice*, Oxford University Press, Oxford, **2014**, 2000.
- [9] a) R. W. Coughlin, M. Aizawa, B. F. Alexander, M. Charles, *Biotechnol. Bioeng.* **1975**, *17*, 515; b) P. Llanes, C. Rodríguez-Escrich, S. Sayalero, M. A. Pericàs, *Org. Lett.* **2016**, *18*, 6292; c) S. B. Ötvös, I. M. Mándity, F. Fülöp, *J. Catal.* **2012**, *295*, 179; d) X. C. Cambeiro, R. Martín-Rapún, P. O. Miranda, S. Sayalero, E. Alza, P. Llanes, M. A. Pericàs, *Beilstein J. Org. Chem.* **2011**, *7*, 1486; e) M. Planchestainer, M. L. Contente, J. Cassidy, F. Molinari, L. Tamborini, F. Paradisi, *Green Chem.* **2017**, *19*, 372.
- [10] D. Simon, F. Obst, S. Haefner, T. Heroldt, M. Peiter, F. Simon, A. Richter, B. Voit, D. Appelhans, *React. Chem. Eng.* **2019**, *4*, 67.
- [11] P. Berg, F. Obst, D. Simon, A. Richter, D. Appelhans, D. Kuckling, *Eur. J. Org. Chem.* **2020**.
- [12] F. Obst, D. Simon, P. J. Mehner, J. W. Neubauer, A. Beck, O. Stroyuk, A. Richter, B. Voit, D. Appelhans, *React. Chem. Eng.* **2019**, *4*, 2141.
- [13] M. Gruttadauria, F. Giacalone, R. Noto, *Chem. Soc. Rev.* **2008**, *37*, 1666.
- [14] H. E. Bigelow, *Chem. Rev.* **1931**, *9*, 117.
- [15] a) D. Campbell, *Dyes Pigm.* **1995**, *29*, 77; b) S. Patai (Ed.) *The chemistry of functional groups. Supplement F*, John Wiley & Sons, Chichester, **1982**; c) B. M. Trost, I. Fleming (Eds.) *Comprehensive organic synthesis. Selectivity, strategy & efficiency in modern organic chemistry*, Pergamon Press, Oxford, **1991**; d) T. Ikeda, O. Tsutsumi, *Science* **1995**, *268*, 1873.
- [16] a) S. B. Waghmode, S. M. Sabne, S. Sivasanker, *Green Chem.* **2001**, *3*, 285; b) A. B. E. Vix, P. Müller-Buschbaum, W. Stocker, M. Stamm, J. P. Rabe, *Langmuir* **2000**, *16*, 10456.
- [17] A. Rezaeifard, M. Jafarpour, M. A. Naseri, R. Shariati, *Dyes Pigm.* **2008**, *76*, 840.

- [18] a) H. Kagechika, T. Himi, K. Namikawa, E. Kawachi, Y. Hashimoto, K. Shudo, *J. Med. Chem.* **1989**, *32*, 1098; b) H. Takahashi, T. Ishioka, Y. Koiso, M. Sodeoka, Y. Hashimoto, *Biol. Pharm. Bull.* **2000**, *23*, 1387.
- [19] a) L. Hou, X. Chen, S. Li, S. Cai, Y. Zhao, M. Sun, X.-J. Yang, *Org. Biomol. Chem.* **2015**, *13*, 4160; b) H. Li, P. Li, Q. Zhao, L. Wang, *Chem. Commun.* **2013**, *49*, 9170; c) H. Li, X. Xie, L. Wang, *Chem. Commun.* **2014**, *50*, 4218; d) D. Zhang, X. Cui, F. Yang, Q. Zhang, Y. Zhu, Y. Wu, *Org. Chem. Front.* **2015**, *2*, 951.
- [20] L. Ke, G. Zhu, H. Qian, G. Xiang, Q. Chen, Z. Chen, *Org. Lett.* **2019**, *21*, 4008.
- [21] A. R. Becker, L. A. Sternson, *J. Org. Chem.* **1980**, *45*, 1708.
- [22] S. S. Acharyya, S. Ghosh, R. Bal, *ACS Sustainable Chem. Eng.* **2014**, *2*, 584.
- [23] S. P. Annen, H. Grützmacher, *Dalton Trans.* **2012**, *41*, 14137–14145.
- [24] Y.-F. Chen, J. Chen, L.-J. Lin, G. J. Chuang, *J. Org. Chem.* **2017**, *82*, 11626.
- [25] Y. Nishiyama, A. Fujii, H. Mori, *React. Chem. Eng.* **2019**, *16*, 10456.
- [26] D. B. Ramachary, C. F. Barbas, *Org. Lett.* **2005**, *7*, 8, 1577–1580C.
- [27] Gebhardt, B. Priewisch, E. Irran, K. Rück-Braun, *Synthesis* **2008**, *2008*, 1889.
- [28] T. E. Kristensen, K. Vestli, K. A. Fredriksen, F. K. Hansen, T. Hansen, *Org. Lett.* **2009**, *11*, 2968.
- [29] R. Toomey, D. Freidank, J. Rühle, *Macromolecules* **2004**, *37*, 882.
- [30] F. Pirani, N. Sharma, A. Moreno-Cencerrado, S. Fossati, C. Petri, E. Descrovi, J. L. Toca-Herrera, U. Jonas, J. Dostalek, *Macromol. Chem. Phys.* **2017**, *218*, 1600400.
- [31] a) T. E. Kristensen, F. K. Hansen, T. Hansen, *Eur. J. Org. Chem.* **2009**, *2009*, 387; b) T. E. Kristensen, K. Vestli, M. G. Jakobsen, F. K. Hansen, T. Hansen, *J. Org. Chem.* **2010**, *75*, 1620.
- [32] W. Lee, T. Mayer-Gall, K. Opwis, C. E. Song, J. S. Gutmann, B. List, *Science* **2013**, *341*, 1225.
- [33] H. A. Zayas, A. Lu, D. Valade, F. Amir, Z. Jia, R. K. O'Reilly, M. J. Monteiro, *ACS Macro Lett.* **2013**, *2*, 327.
- [34] A. Córdova, W. Zou, P. Dziedzic, I. Ibrahim, E. Reyes, Y. Xu, *Chem. Eur. J.* **2006**, *12*, 5383–5397.
- [35] K. G. Orrell, V. Šik, D. Stephenson, *Magn. Reson. Chem.* **1987**, *25*, 1007.
- [36] D. Beaudoin, J. D. Wuest, *Chem. Rev.* **2016**, *116*, 258.
- [37] Y. Hayashi, J. Yamaguchi, T. Sumiya, M. Shoji, *Angew. Chem. Int. Ed.* **2004**, *43*, 1112–1112; *Angew. Chem.* **2004**, *116*, 1132–1135
- [38] Z. Liu, Y. Huang, Q. Xiao, H. Zhu, *Green Chem.* **2016**, *18*, 817.
- [39] a) S. Ghosh, S. S. Acharyya, T. Sasaki, R. Bal, *Green Chem.* **2015**, *17*, 1867. b) B. Paul, S. K. Sharma, S. Adak, R. Khatun, G. Singh, D. Das, V. Joshi, S. Bhandari, S. S. Dhar, R. Bal, *New J. Chem.* **2019**, *43*, 8911.
- [40] B. Priewisch, K. Rück-Braun, *J. Org. Chem.* **2005**, *70*, 2350.
- [41] T. Majima, W. Schnabel, W. Weber *Makromol. Chem.* **1991**, *192*, 2307–2315.

Manuscript received: January 4, 2021
Revised manuscript received: February 22, 2021
Accepted manuscript online: February 24, 2021